Toxicology Research

Palmitic acid induced lipotoxicity is associated with altered lipid metabolism, enhanced CYP 450 2E1 and intracellular calcium mediated ER stress in human hepatoma cells

Journal:	*Toxicology Research*
Manuscript ID:	TX-ART-04-2015-000101.R1
Article Type:	Paper
Date Submitted by the Author:	12-Jun-2015
Complete List of Authors:	Ashraf, Nissar; Indian Institute of Integrative Medicine, PK-PD and Toxicology Division Sharma, Love; Indian Institute of Integrative Medicine, PK-PD and Toxicology Tasduq, Sheikh; CSIR-Indian Institute of Integrative Medicine, PK-PD and Toxicology Division

Palmitic acid induced lipotoxicity is associated with altered lipid metabolism, enhanced CYP 450 2E1 and intracellular calcium mediated ER stress in human hepatoma cells.

Ashraf Ul Nissar[1,2], Love Sharma[1,2], Sheikh A Tasduq[1,2*]

[1]Academy of Scientific and Innovative Research (AcSIR), New Delhi, India

[2]PK-PD and Toxicology Division, CSIR-Indian Institute of Integrative Medicine, Canal Road, Jammu Tawi, Jammu and Kashmir, India.

[*]PK-PD and Toxicology Division,
CSIR-Indian Institute of Integrative Medicine,
Council of Scientific and Industrial Research (CSIR)
Canal Road
Jammu Tawi
Jammu and Kashmir
India.
E-mail: stabdullah@iiim.ac.in; tasduq11@gmail.com
Phone: +91-1912569000-10-Ext-332

Abstract:

The aim of the present investigation was to study the events associated with palmitic acid induced metabolic and lipotoxic changes in human hepatoma cells (Hep3B, Huh7 and HepG2). The cells were lipid overloaded with varied concentrations of saturated fatty acid (Palmitic acid). It was observed that (a) SFA induced significant metabolic changes including CD36/FAT, SREBP1, PPARγ and SCD1 upregulation and decreased *Mtt*p levels in HepG2 and Huh7 cells but not in Hep3B cells. (b) the toxic manifestations including changes in Ca^{2+} levels, mitochondrial dysfunction and activation of PERK-eIF2α-CHOP pathway due to SFA were more pronounced in Huh7 and Hep3B as compared to HepG2 cells; (c) induction of CYP2E1 and oxidative stress by SFA was observed in all three hepatoma cells. Interestingly, CYP2E1 over expressing cells (E47 cells) were found to be significantly sensitized towards lipotoxicity; and (d) Metabolic and toxic manifestations including altered blood biochemistry, ER stress and CYP2E1 induction were evident in C57BL/6J mice fed with a diet rich in cholesterol and saturated fatty acids (2%-cholesterol/12% SFA-HC/HF) for 16 weeks (model used to confirm the key events taking place in in vitro system). Histopathological analysis of livers of HC/HF fed mice showed micro and macro-vesicular steatosis, hepatocyte ballooning, infiltration of neutrophils and prominence of Kupffer cells. In conclusion our data suggests that Palmitic acid alters lipid metabolism, causes oxidative stress and disturbs intracellular Ca^{2+} balance that terminates in CYP 2E1 induction, ER stress and lipoapoptosis.

Key words: Lipotoxicity; ER Stress; Mitochondrial dysfunction; oxidative stress; SREBP1;CD36; Mttp; CYP2E1

Abbreviations:

NAFLD: Non Alcoholic Fatty Liver Disease,
NASH: Non Alcoholic steatohepatitis
SFA: Saturated fatty acids
SREBP1: Sterol Regulatory Element Binding Protein 1
PERK: PKR like ER Kinase
CYP2E1: Cytochrome P 2E1
ΔΨm: Mitochondrial membrane potential
GRP78: Glucose regulated protein 78
GADD34: Growth arrest and DNA damage 34
CHOP: C/EBP homologous protein
PUMA: P53 upregulated modulator of apoptosis
Mttp: Microsomal triglyceride transport protein
SCD1: Stearoyl CoA desaturase 1
CD36/FAT: Fatty acid Translocase
CYP2E1: Cytochrome 450 2E1
ROS: Reactive oxygen species
HC/HF: High cholesterol and High Fat

Introduction

Prevalence of non-alcoholic fatty liver disease (NAFLD) has been on an inclined trajectory with the rise in obesity and has been found to be affecting about 50% of individuals in some populations.[1] Non alcoholic steatohepatitis (NASH), an advanced stage of NAFLD has emerged as third most common cause of liver transplantation in United States of America.[2] NAFLD can progress to cirrhosis and liver failure in 3% to 15% cases and there have been emerging reports of a significant proportion of HCC cases in settings of NAFLD.[3] Despite the high prevalence of NAFLD and its serious complications the underling molecular events that implicate lipotoxicity remain poorly understood and need further investigation.

The basic events involved in the pathogenesis of NAFLD are the increased activity of SREBP-1, ChREBP-1 and PPARγ, elevated ROS production, increased fatty acid influx, suppressed fatty acid oxidation due to CPT-1 inhibition and altered lipoprotein assembly and secretion.[4] Lipid droplet formation and the subsequent lipotoxicity result from alterations in multiple cellular events but are far from clear. Many recent studies have shown that saturated fatty acids caused greater lipotoxicity than unsaturated fatty acids and it has been shown that partitioning of fatty acids between saturated and unsaturated determines the lipotoxicity.[5] The uptake and synthesis of fatty acids is considered as one of the important cellular steps in the pathogenesis of NAFLD and is controlled by specific transporters such as CD36, fatty acid binding protein (FABP) and fatty acid transport protein (FATP). In NASH patients, it has been reported that apoptosis is associated with CD36/fatty acid Translocase upregulation,[6] clearly implicating that impaired or increased influx of free fatty acids across hepatocytes is involved in the pathogenesis of NAFLD. Increased influx of fatty acids and glucose is associated with increased lipid droplet formation, oxidative stress and induction of CYP2E1.[7-9] However the molecular events underlying these events remain poorly understood and often controversial.

Deleterious effects of CYP2E1 leads to mitochondrial dysfunctioning and cellular demise.[10] Mitochondrial damage represents a common early event in cellular injury caused by free fatty acids that is manifested by oxidative stress, decrease in $\Delta\Psi m$ followed by ATP depletion and bioenergetic failure.[11] Depletion of intracellular calcium stores due to oxidative stress has been linked to cytoskeleton network disruption and activation of catabolic enzymes leading to cell death.[11] Further Palmitic acid induces ER stress and lipoapoptosis in hypothalamic neurons via c-Jun N-terminal kinase (JNK) dependent pathway.[12] SFA are known to induce the transcription factor CCAAT/enhancer binding homologous protein (CHOP/GADD153) in liver cells that mediates the cellular demise by regulating the death receptor DR5 and BH3 only protein Bim.[13, 14] It

remains elusive what causes ER stress and whether ER stress contributes to hepatocyte steatosis and leads to development of metabolic disorders or it is an adaptive response to restore hepatocyte function. The three important human liver derived cells based models to study molecular mechanism of lipotoxicity are HepG2,[15] Huh-7 and Hep3B.[16] The animal and cell culture based models of lipotoxicity, that have been developed and used in recent years to unravel the molecular mechanisms involved in implicating the lipotoxicity, only mimic certain disease aspects and markedly differ in regards to the degree of hepatocellular damage and metabolic alterations associated with the development of the disease.[17] The aim of the present investigation was to evaluate several cellular and molecular aspects related to metabolic changes and toxic manifestations induced by saturated fatty acid in human hepatoma cells leading to cellular demise. For this purpose, three human hepatoma cells (HepG2, Hep3B and Huh7) were exposed to varied concentrations of saturated fatty acid for varied time periods and cytotoxicity, intracellular Ca^{2+} levels, ROS, ER stress, lipoapoptosis and factors related to lipid droplet formation and its traffic across hepatocytes were evaluated. Further, individually caged C57BL/6J mice fed with HC/HF diet (sedentary life style) were employed to confirm the key cellular events with regards to metabolic alterations and toxic manifestations using biochemical and histological analysis.

This is the first report that suggests the comparative lipotoxic profile of SFA on three different human liver derived cell types (Hep3B, Huh7 and HepG2) presenting the cellular and molecular hallmarks of lipotoxicity as evident in clinical NAFLD. Importantly our data suggests the importance of CYP2E1 and metabolic changes with regards to SCD1, CD36 and microsomal triglyceride transfer protein (*Mttp*) as important determinants of lipotoxicity in NAFLD.

Materials and Methods

Cell Culture and Fatty Acid Treatment:

HepG2 and Hep3B cells were procured from ATCC USA. Huh7 cell line was obtained from Professor Michael Charlton, Department of Gastroenterology and Hepatology, Mayo Clinic, Rochester, USA. Cells were grown and maintained in Dulbecco's Modified Eagle's Medium containing L-Glutamine, glucose (3.5g/L), 15mM Hepes, 200U/mL Penicillin, 270µg/mL Streptomycin and 10% (v/v) Fetal bovine serum (FBS), obtained from Sigma Aldrich, St. Louis, MO at 37^{o}C in a humidified atmosphere of 5% CO_2. Two sublines of human hepatoma HepG2 derived cells as described by Cederbaum (1998) were used, i) E47 cells, which constitutively express human CYP2E1, and ii) C34, which are HepG2 cells transfected with empty pC1 vector (For expression analysis, refer to Supplement figure II). E47 and C34 cell lines were obtained as a kind gift from Professor

Arthur I Cederbaum, Department of pharmacology and systems therapeutics, Mount Sinai School of Medicine, NY USA. For all experiments cells were used at density of 0.7 x 10^4 cells/96 well plate, 7 x 10^5 cells/6 well plate or 1.2 x 10^6 cells/60mm dish. All the studies were conducted using 70-80% confluent cells, which were treated with indicated concentrations of Palmitic acid.

Animal Treatment:

Male C57BL/6J mice aged 6-8 weeks were maintained in individual cages (1 mouse/cage for sedentary life,[18]) and had free access to water and standard chow for about one week before the start of experiment. Animals were randomly divided into two groups (10 animals per group) with one group receiving standard chow and other group receiving diet containing 12% SFA and 2% Cholesterol (HC/HF) for 4 months (16 weeks). High fructose corn syrup (HFCS, 42g/L final concentration) was administered in drinking water of HC/HF group (*Anuradha Krishnan, Tasduq Abdullah, Toafic Mounajjed, Stella Hartono, Andrea L. McConico, Thomas A. White, Ian Lanza, Nathan K. LeBrasseur, K Sreekumaran Nair, Gregory J. Gores, Michael Charlton. Dynamics of Hepatic Lipid Composition, and Mitochondrial Function during the Evolution of Fast Food-Induced NASH – From the First Mouthful to Steatofibrosis. Hepatology, Vol 60. No. 4 (Supplement), pp 732A, Abstrace No. 1093, October 2014*). The diet was obtained as a kind gift from Professor Michael R Charlton, Mayo Clinic, Rochester USA. At 4 months, mice were euthanized by CO_2 inhalation, blood was drawn by cardiac puncture, livers were excised, cut in pieces and kept for protein extraction as frozen tissue or preserved in 10% formalin for tissue histochemistry. All the animal procedures were performed according to the guidelines for Animal Care and Use committee of Indian Institute of Integrative Medicine (CSIR) which reviewed and approved all the protocols. The detailed composition of diet is presented in supplement Figure I.

Blood Biochemistry and Pathology Assessment:

Serum glucose, triglycerides and cholesterol were measured using commercially available kits as per the manufacturer's instruction (Erba, Mannheim Germany). Insulin ELISA kit (mouse) was obtained from Millipore, Billerica, MA, USA. Formalin fixed liver sections were embedded in paraffin and sectioned (4μm). Sections were stained with Picro sirus and H&E to examine the general morphology. Slides were assessed by experienced liver pathologist (Dr. B. C Subash) who was blinded to the study.

FFA-BSA Complex Preparation:

20% stock solution of fatty acid free BSA (A6003, Sigma Aldrich, St. Louis, MO) was prepared by dissolving 750mg of BSA in 3.75 mL PBS (pH 7.4). To begin with, BSA was layered on top of the 2-2.5mL PBS. BSA was allowed to dissolve on its own (without stirring) at 4^{o}C. The final volume was adjusted to 3.75mL. For

20mM Palmitic acid solution, 5.6mg of sodium palmitate was added to 1mL water pre-heated to 70^{o}C. The mixture was incubated at 70^{o}C for 20-30 minutes with constant vortexing. FFA-BSA complex was prepared by mixing 1mL of 20mM sodium palmitate solution to 3.3 mL of 20% BSA (pre-warmed at 37^{o}C). Complex formed was immediately added to 15.7mL DMEM pre-warmed to 37^{o}C. Final solution prepared had 1mM Palmitic acid. Solution was sterile filtered and remains stable for about one week at 4^{0}C.

3-(4,5-Dimethylthiazol-2-yl)-2,5-diphenyltetrazolium bromide (MTT) Assay:

In vitro Cytotoxicity test was done to identify the cytotoxic potential of Palmitic acid[19]. HepG2, HuH7, Hep3B, C34 and E47 cells were seeded in 96 well plate and treated with different concentrations of Palmitic acid. After 24 hours medium was removed and the cells were incubated in fresh medium without serum, containing 250ug/mL MTT for 3 hours at 37^{0}C. Cytotoxicity/Cell viability was evaluated by assaying the ability of mitochondria to catalyze the reduction of thiazolyl blue tetrazolium bromide (MTT) to a formazan salt by mitochondrial dehydrogenases.

Nile Red Staining:

Nile red, a lipophillic dye was used to assess fat accumulation in hepatocytes. HepG2, HuH7 and Hep3B cells were treated with different concentrations of Palmitic acid for 24 hours. Cells were washed with PBS and fixed in Methanol:Acetic acid (3:1) solution overnight at 4^{0}C. Cells were washed and incubated in PBS containing 500ng/mL Nile red (Sigma Aldrich, St. Louis, MO) for 30 minutes at 37^{0}C. Imaging was done by fluorescence microscope (Nikon TE2000U, Tokyo, Japan) using green filters. For FACS analysis Cells were collected, fixed in Methanol: Acetic acid (3:1) solution overnight at 4^{0}C and resuspended in PBS containing 500ng/mL Nile red. Cells were incubated at 37^{0}C for 30 minutes. Analysis was done by BD FACS caliber Flow Cytometer. Instrument settings were adjusted using unstained cells.

Protein Isolation and Western blotting:

Cells were trypsinised, harvested in PBS (pH 7.4), centrifuged and resuspended in RIPA buffer. After incubation for 45 minutes at 4^{0}C, lysate was centrifuged at 14,000 rpm for 30 minutes at 4^{0}C to remove cellular debris. Tissue lysates were prepared by homogenising tissue samples in lysis buffer (50mM Tris, 150mM NaCl, 1mM EDTA, 1% sodium deoxycholate, 0.1% SDS, 1% IGEPAL, 1% protease inhibitor Cocktail). Protein concentrations were determined by Bradford assay. For western blotting 30-50 µg protein were denatured at 100^{0}C for 3 minutes in Laemmli Buffer. Protein Samples were resolved on 7%-12% SDS gels at 70V. Proteins were electro-transferred to PVDF membrane (BioRad, Hercules, CA) using BioRad Mini Transblot Electrophoretic transfer Cell. Membranes were blocked in 5% fat free dry milk in 50mM Tris, pH 8.0 with

150mM sodium chloride, 2.6mM KCl and 0.05% Tween 20 for 2 hours. Rabbit: anti-SREBP1, anti-CD36, anti-Bcl2, anti-Bim, anti-PARP1, anti-PUMA, anti-GRP78, anti-CHOP/GADD153, anti-ATF4, anti-GADD34, Goat: anti-Caspase 3, anti-*Mttp*, (Santa Cruz Biotechnologies, CA), rabbit anti CYP450 2E1 (Calbiochem, Darmstadt Germany), anti-SCD1 (Cell Signalling Technology, Danvers, MA) mouse anti-β actin (Sigma Aldrich, St. Louis, MO) antibodies were used as primary antibodies in fat free milk overnight at 4^0C. Goat anti-rabbit, goat anti-mouse and rabbit anti-goat immunoglobulin G antibodies conjugated with HRP (Santa Cruz Biotechnologies, CA) were used as secondary antibodies. Chemiluminiscence was detected by Immobilon chemilumniscent HRP substrate (EMD- Millipore, Billerica, MA) and visualised by Molecular Image ChemiDoc^{TM} XRS^{+} (Bio-Rad, Hercules, CA). Densitometric measurement of the bands was performed using Image Lab^{TM} software version 3.0 (Bio-Rad, Hercules, CA).

Determination of Reactive Oxygen Species:

ROS assessment was done as described previously.[20] Briefly, HepG2, HuH7 and Hep3B cells were seeded in 6 well plates. After corresponding treatments for 24 hours, cells were washed three times with PBS and fresh medium containing 5μM H_2DCF-DA was added. Cells were incubated for 30 minutes at 37^0C. Cells were again washed three times with PBS and imaged under a thin film of PBS. Imaging was done by fluorescence microscopy (Nikon TE 2000U, Tokyo, Japan) using green filters.

Intracellular Ca^{2+} release and ΔΨm study:

Fluo3 AM, a Ca^{2+} probe was used to measure intracellular Ca^{2+} in hepatocytes. Cells were grown on sterilised cover slips. After Corresponding treatment of Palmitic acid for 4 hours, fresh medium containing 5μM Fluo3 AM was added. Cells were incubated for 30 minutes at 37^0C and 5% CO_2. Cells were washed three times with PBS (pre warmed at 37^oC) and slides were prepared for Confocal microscopy and imaging was done using laser scanning Confocal microscope (Olympus FluoView FV 1000) with 488 laser line as described.[21] For ΔΨm study cells were stained with JC-1(5μg/mL) and imaging of cells was done according to an established protocol.[22] Briefly, cells were cultured on sterile cover slips. At about 50-60% Confluence cells were treated with different concentrations of Palmitic acid. After 12 hours fresh medium pre warmed to 37^0C containing 5μg/mL JC-1 (Sigma Aldrich, St. Louis, MO) was added to cells and incubated for 30 minutes at 37^0C in a CO_2 incubator. Medium was removed and cells were washed three times with PBS (pre warmed at 37^0C). Cover slips were mounted on slides, sealed and imaging was done using laser scanning Confocal microscope (Olympus FluoView FV1000) with excitation at 488nm and dual emission at 525/590nm for red/green fluorescence respectively.

Statistical analysis.

Data are presented as mean ±SD from three independent experiments. Statistical comparisons between the groups were determined by using one-way ANOVA followed by Dunnett's test using Primer of Biostatistics, version 4.0 (McGraw Hill). $p<0.05$ was considered as statistically significant.

Results:

Free fatty acid treatment induces hepatic steatosis, lipotoxicity and differential induction of Stearoyl-CoA desaturase 1 in hepatocytes:

We first confirmed our cell culture models for lipid accumulation by treating HepG2, Hep3B and Huh7 cells with different concentrations of free fatty acid in DMEM. All the models accumulated lipid droplets. Lipid droplet (neutral lipids) formation as indicated by yellow gold fluorescence in HepG2 was greater as compared to Hep3B and Huh7 cells. These results recapitulate lipid accumulation, as an essential feature of SFA treatment (Figure 1A). The toxicity of Palmitic acid was found to be concentration dependent in all the cell types tested. Hep3B and Huh7 cells showed more sensitivity towards free fatty acids as compared to HepG2 Cells. In HepG2 cells treated with 0.25mM and 0.5mM Palmitic acid, the toxicity was 18% and 23% respectively, toxicity was minimal below 0.25mM of Palmitic acid treatment. Hep3B cells showed significant toxicity of 18%, 26% and 36% at 0.1mM, 0.25mM and 0.5mM respectively. In case of Huh7 cells, the toxicity was 19%, 24% and 32% at 0.1mM, 0.25mM and 0.5mM Palmitic acid respectively (Figure 1B). E47 cells (CYP2E1 over expressing cell line) showed significantly higher lipotoxicity as compared to its control cell line, C34 (Figure 1C). Mouse hepatocyte AML12 (normal mouse hepatocyte) was also employed for cell viability evaluation. AML12 also showed concentration dependent decrease in cell viability. (Supplement Figure II). Oleate was used as non toxic fatty acid and there was no significant cytotoxic effect of oleate in any of the three cells lines used (data not shown). HepG2, Huh7 and Hep3B cells were tested for the induction of SCD1 protein on exposure of Palmitic acid. HepG2 showed almost 2 fold induction of SCD1 at 0.5mM Palmitic acid after 24 hours whileas Hep3B and Huh7 showed no induction of SCD1 (Figure 1D). SCD1 has been shown to play protective role and is considered as a potential oncogene and may play role in comparative protection against Palmitic acid in HepG2 cells.

HC/HF mice develop metabolic changes, altered blood biochemistry and liver injury characteristic of NAFLD and NASH:

Weight gain was significantly (*$p<0.05$) higher in HC/HF mice, compare to mice fed with standard chow over a period of 16 weeks. HC/HF mice had elevated levels of serum glucose, triglycerides, cholesterol and Insulin at

16 weeks as compared to SC mice (Figure 1E). The photomicrograph of section of liver from control mice showed normal lobular architecture whereas HC/HF mice showed micro and macro vesicular steatosis, ballooned hepatocytes, kupffer cell prominence and inflammation (Figure 1F). Expression of PPARγ and CD36 was increased in livers of HC/HF mice as compared to SC mice (Figure 2B). The results from the in vivo model presented here are to confirm the key events taking place in in vitro system.

SREBP1 and PPARγ Over expression induced by Palmitic acid is associated with CD36 upregulation and downregulation of M*tt*P leading to impaired influx and efflux of fat in hepatocytes.

Transcription factors SREBP1 and PPARγ responsible for lipogenesis were upregulated in Palmitic acid treated hepatocytes. Protein expression studies showed little significant change in levels of SREBP1 and CD36 in Huh7 at 0.25mM. The decrease in protein levels above 0.25mM can be attributed to cytotoxicity induced by palmitic acid. Hep3B cells does not show any significant change even at 0.25mM in these metabolic players, whileas HepG2 cells showing good amount of change in these metabolic players. The cells showed almost two fold increase in spliced form of SREBP1 at 0.5mM Palmitic acid treatment group and 1.5 fold increase in CD36 levels. PPARγ levels were also increased in Palmitic acid treated cells, although not as significant as SREBP1. Further western blotting results of M*tt*p revealed a significant and concentration dependent decrease in M*tt*p levels. Quantitatively, protein levels of M*tt*p decreased by 1.3 fold and 1.8 fold at 0.5mM and 1mM Palmitic acid in Huh7 whileas HepG2 showed 1.2 and 1.9 fold decrease respectively (Figure 2A).

Intracellular Ca^{2+} levels in *In vitro* models and generation of Endoplasmic reticulum stress in hepatocytes and HC/HF mice:

As mentioned above in the cell viability results, HepG2 was comparatively resistant to palmitic acid lipotoxicity, we decided to study the majority of lipotoxic parameters in Hep3B and Huh7 only. Confocal microscopy results reveal that Palmitic acid treatment in Hep3B and Huh7 cells caused a concentration dependent increase in intracellular Ca^{2+} levels (Figure 3A). ER stress was evident, as main players of UPR were upregulated as revealed by the expression of ATF4, CHOP/GADD153 and GADD34. Huh7 cells showed 3 fold increase in CHOP levels at 0.5mM Palmitic acid and 1.7 fold increase in ATF4 after12 hours of Palmitic acid exposure whereas Hep3B cells showed 1.6 and 1.4 fold increase in CHOP and ATF4 levels respectively. HepG2 cells showed no significant difference in these proteins between control and treated cells (data not shown). Endoplasmic reticulum stress was evident in HC/HF mice as markers of ER stress were upregulated. GRP78 increased by 3 fold whereas CHOP/GADD153 increased by 1.4 fold in livers of HC/HF mice as compared to SC mice (Figure 2B, 3B and 3C). The decrease in the levels of proteins can again be attributed to cytotoxic effects

of Palmitic acid (eg: at 1mM palmitic acid, HuH7 cells showed almost 55-60% cytotoxicity). Thapsigargin was used as positive control to induce ER stress, although the impact was little. Since ER stress plays important role in cell death, we tried to study effect of inhibition of ER stress by a chemical chaperone, 4 phenylbutyric acid on cell viability in palmitate treated cells. The results showed that pre treatment of 4PBA in palmitate treated cells significantly restored the cellular viability in palmitate treated cells (40-50% restoration). These results clearly show that ER stress developed due to imbalance in Ca^{2+} homeostasis in palmitate treated cells does play important role in cell death.

Palmitic acid induced Loss of Mitochondrial membrane potential:

Exposure of cells to Palmitic acid induced marked change in ΔΨm as evident by disappearance of red fluorescence in most of the cells. At 1mM Palmitic acid, significant cell population was found to be devoid of red fluorescence which indicates the loss of ΔΨm and severity of the damage. Treatment of cells with Camptothecin (used as positive control) increased green fluorescence and mitochondria were seen as clusters. Loss of ΔΨm in HepG2 cells was associated with significant vacuolisation of cytoplasm and nuclear condensation thus giving an insight that Type II cell death (Autophagy) precedes Type I cell death (apoptosis) in HepG2 cells upon exposure to Palmitic acid (Figure 4). These results clearly reveal that mitochondrial permeability transition induced by Palmitic acid collapses the electrochemical gradient across the mitochondrial membrane as measured by ΔΨm.

CYP2E1 induction, Oxidative stress and lipoapoptosis:

There was an increased induction of CYP2E1 levels on exposure to Palmitic acid for 24 hours. CYP2E1 levels showed 1.4 fold increase at 0.25mM Palmitic acid in Hep3B cells whereas HepG2 cells showed 1.3 and 1.7 fold increase in CYP2E1 levels at 0.25mM and 0.5mM Palmitic acid respectively. Huh7 cells showed almost 3 fold increase of CYP2E1 levels at 0.25mM and 0.5mM Palmitic acid. No further significant change was observed in Hep3B cells at 0.5mM and higher concentrations of Palmitic acid. Livers of HC/HF mice showed 1.4 fold increased expression of CYP2E1 as compared to mice fed with SC (Figure 5). Fluorescence microscopy results show increased amount of intracellular ROS as demonstrated by increased fluorescence in all cell types after treatment with different concentrations of Palmitic acid (Figure 5). Further molecular players controlling antioxidant defence/response system within cells were studied by western blotting in Huh7 cells. The results clearly revealed impairment in the system as important proteins like Nrf2 and SOD1 were downregulated due to palmitate treatment. However, expression of Catalase showed no significant change. There are enough previous reports suggestive of the fact that free fatty acids lead to cell death in a caspase dependent manner.[5, 16, 23] We

also performed immunoblotting and results clearly reveal apoptosis as determined by the PARP1/2 cleavage in Palmitic acid treated Hep3B and Huh7 cells. Anti-apoptotic Bcl-2 down regulation and upregulation of pro-apoptotic PUMA was also evident in these cells (Figure 6). There was no change in PUMA in Hep3B as the cells are P53 null. (data not shown). Furthermore, PARP1 cleavage and cell death induced by Palmitic acid were also analysed and confirmed in non transformed cell line, AML12. (Supplement Figure II).

Discussion:

Principal findings of study relate to the mechanisms linking increased influx of free fatty acids into hepatocytes to lipotoxicity and cellular demise. The results of present study demonstrated that exposure of hepatocytes (HepG2, Huh-7 and Hep3B) to SFA induces overexpression of SREBP1 and CD36 causing increased influx of fatty acids into hepatocytes which is further associated with decreased levels of *MttP* causing decreased hepatic lipid clearance. Further SFA treatment to hepatocytes resulted in emptying of ER Ca^{2+} stores and hence inducing ER stress which is further associated with generation of reactive oxygen species, increased CYP2E1 levels and loss of mitochondrial membrane potential, thereby starting a cascade leading to caspase activation and finally lipoapoptosis. The *In vivo* study revealed that mice exposed to HC/HF for a period of 16 weeks develop a broad spectrum of NAFLD related metabolic and histological changes including micro and macro vesicular steatosis, hepatocyte ballooning, foci of steatohepatitis, prominence of kupffer cells, ER stress and CYP450 2E1 induction.

Our cell culture models of lipotoxicity showed significant steatosis and lipotoxicity in hepatocytes (Figure 1A, 1B and 1C). Hep3B and Huh7 showed more sensitivity towards lipotoxic effects of Palmitic acid as compared to HepG2 cells. This degree of protection in HepG2 in comparison to Hep3B and Huh7 may be attributed to the Stearoyl-CoA desaturase 1 (Figure 1D) which is protective in nature[24] and plays important role in hepatic lipid partitioning and liver damage in NAFLD.[5] Molecular events that result in the intrahepatic lipid accumulation and growth of lipid droplets are poorly understood, but may arise from several reasons like increased uptake, elevated de nova synthesis, reduced fatty acid oxidation and/or diminished efflux involving impaired lipoprotein synthesis or secretion.[25, 26] Increased expression/activity of nuclear receptor PPARγ is germane to the growth of lipid droplets and is physiologically stimulated by fatty acids.[4] Our data clearly shows that Palmitic acid exposure to HepG2 cells resulted in increased expression of PPARγ coinciding with increased activity of SREBP1 (Figure 2A). This results in increased lipogenesis and lipid accumulation in hepatocytes. Upregulation of PPARγ and SREBP1 was found to be associated with increased expression of CD36 resulting in enhanced uptake of fatty acid by hepatocytes. As fat accumulation sets in, hepatocytes transport excessive lipids into

mitochondria for β-oxidation or arranges for its removal as lipoprotein complex. Very low density lipoprotein (VLDL) is one of the five major groups of lipoproteins that facilitate hepatic lipid clearance. VLDL synthesis depends on the Microsomal triglyceride transport protein (M*tt*P) activity.[27] Inhibition of activity of M*tt*P has been considered as one of the contributing factors to lipid accumulation in alcoholic steatosis,[28] hepatitis C related steatosis[29] and drug induced steatosis.[30] Therefore M*tt*P is one of the risk factors for development of steatosis and NASH. Our immunoblotting results showed concentration dependent decrease in M*tt*P levels, suggesting the role of M*tt*P in development of Palmitic acid induced fat accumulation in hepatocytes (Figure 2A). These results clearly reveal that Palmitic acid induces upregulation of PPARγ, SREBP1 and CD36 and downregulation of M*tt*P. Collectively there is an increased uptake of fatty acids, lipid droplet formation and failure of VLDL to assemble. This results in retention of lipids in hepatocytes (steatosis). All these events lead to development of '*first hit'* (fat accumulation) and herein experimentally demonstrated in HepG2 cells. It is worth mentioning that Hep3B and Huh7 cells do not show any significant change in SREBP1 and CD36 proteins as compared to HepG2 cells but show more pronounced toxic manifestations. This suggests that HepG2 can be a good model to study lipid metabolic studies whileas Hep3B and Huh7 can be employed in lipoapoptotic studies due to SFA exposure. Further livers of HC/HF mice had increased expression PPARγ and CD36 and NAFLD/NASH characteristics as mentioned above (Figure1E, 1F and 2B). These results clearly showed that metabolic changes as observed in clinical NASH could be reproduced in *In vitro* as well as *In vivo* model of lipotoxicity.

Endoplasmic reticulum is a signalling organelle possessing ability to release sequestered Ca^{2+} ions through ion channels that respond to various stimuli.[31] Disruption in the Ca^{2+} homeostasis within ER lumen causes protein unfolding and misfolding, triggering an evolutionary conserved response to maintain homeostasis known as Unfolded Protein Response (UPR). If homeostasis cannot be re-established, cell death is triggered.[32] ER stress has been linked to PUMA induction during SFA mediated lipotoxicity.[33] Plethoric evidence exist regarding SFA induced ER stress but underlying cause and mechanisms remains elusive. We tried to answer the question and our results link SFA induced ER stress to disturbance of Ca^{2+} homeostasis in ER lumen leading to activation of UPR. Confocal microscopy results revealed increase in intracellular Ca^{2+} levels, as a consequence of Palmitic acid exposure (Figure 3). Since ER is the major Ca^{2+} pool in the cell and there are evidences suggesting that the Ca^{2+} pools within a cell can be functionally heterogeneous, however it is ER or the sub-fractions thereof, which constitute a highly significant portion of Ca^{2+}-pools of the cell and functions to provide the source of cytosolic Ca^{2+} signals.[34] Disruption of Ca^{2+} homeostasis in ER lumen leads to Ca^{2+} overload in cytoplasm and activation

of PERK-eIF2α-CHOP pathway (Figure 3). ER stress markers GRP78 and CHOP/GADD153 were also upregulated in livers of HC/HF mice. Further Palmitic acid was shown to induce loss of ΔΨm (Figure 4). Both processes are related: mitochondria posses large ability for Ca^{2+} uptake which is carried out by potential-driven calcium uniporters and Ca^{2+} uptake into mitochondria consumes membrane potential and produces depolarisation.[11] As Ca^{2+} overload is related to mitochondrial dysfunction, it is the disturbances in Ca^{2+} homeostasis that caused the loss of ΔΨm. Hence a link has been drawn between ER stress and mitochondrial dysfunction. Our results clearly reveal Ca^{2+} overload in cytoplasm and disruption of ΔΨm in Palmitic acid treated cells (Hep3B and Huh7). However, HepG2 cells remained relatively protected against SFA induced ER stress and hence lipoapoptosis. This can be credited to the efficient ability of HepG2 cells to convert SFA to less toxic unsaturated fatty acids, due to a significant induction of SCD-1 in HepG2 cells compared to Huh7 and Hep3B.

In alcoholic and obese subject, levels of CYP2E1 are found to be elevated resulting in high ROS production and mild to moderate cellular injury. When these subjects are exposed to xenobiotics that are metabolised by CYP2E1, cellular injury worsens due to overproduction of ROS and reactive metabolites.[10] Our results show elevated levels of both CYP2E1 and ROS in Palmitic acid treated cells (Figure 5). So Palmitic acid treatment in hepatocytes results in development of oxidative burden and disturbance of redox balance leading to ROS accumulation, downregulation of anti-oxidant defence/response element and release of inflammatory cytokines, *a second hit* (confirmed by IL-6 release, Supplement Figure III). CYP2E1 regulates the oxidative burden and has been shown to play important role in the carcinogenesis.[35] Present result shows the induction of CYP2E1 both in *In vitro* conditions (HepG2, Huh7 and Hep3B) and in livers of HC/HF mice, which may play role in the development of hepatocellular carcinoma and also distinguishes steatohepatitis from simple steatosis in NAFLD patients.[36] Previous studies have shown that CYP2E1 over expression potentiates the cellular injury on exposure to drugs or toxins.[19, 37] Our study provides the evidence that CYP2E1 over expression worsens the cellular injury and hastens the cellular damage due to Palmitic acid exposure as shown by enhanced toxicity in E47 cells as compared to C34 cells (Figure 1). Taken together, our results clearly show, CYP2E1, is a potential marker for lipotoxicity and steatohepatitis in both *In vitro* and *In vivo* conditions.

Finally apoptotic parameters (Figure 6) were studied and results clearly show induction of mitochondrial outer membrane permeabilisation (MOMP) due to Palmitic acid treatment and most probably due to CYP2E1 and increased Ca^{2+} that leads to the emergence of pro-apoptotic mediators in the cytosol starting a cascade of events that leads to cell death.

In summary current study provides an insight and uncovers a pathogenic link between nutritional intake (hepatic lipid overloading) and liver injury and confirms a role of cellular disparity in various cell based models of lipotoxicity. The present results support use of multiple models to study lipotoxicity and associates increased influx of free fatty acids with increased intracellular Ca^{2+} levels, CYP2E1, ER stress and cascade of events within the cell leading to lipid droplet formation and cellular death (Figure 7). Further HC/HF diet has been shown to provide the pathopysiological disturbances mimicking human NASH. Our study demonstrated that combinatorial effects of cholesterol, saturated fatty acids, high fructose corn syrup and sedentary lifestyle without any genetic manipulation or use of toxin in C57BL/6J mice sufficiently replicates the features seen in human disease. So based on the findings in this study, we propose that SCD1, *Mttp* and CYP2E1 as important determinants of lipotoxicity and disease progression in NAFLD. Further, on the basis of data derived from various hepatoma cells (HepG2, Huh7 and Hep3B) used, we are of the opinion that HepG2 is a better model to address the lipid droplet formation (steatosis) and metabolic parameters whileas Huh7 and Hep3B are better models to study toxic manifestations due to SFA exposure. Since there is no drug available to treat the NAFLD, therefore it is very important to restrict the calorie intake and increase physical movement to prevent the accumulation of fat in liver and further fibrosisng of NAFLD. Also CYP2E1 inhibitors and curbing of metabolic changes with respect to SCD1 and M*tt*P could be tried for the management of lipotoxicity. A greater understanding of the complex inter-relation between molecular players may lead to development of pharmacologic agents that can curb the disease progression.

Acknowledgements.

We are grateful to Dr. Ram A. Vishwakarma, Director of this institute for supporting the study, Professor Arthur I Cederbaum for providing the C34 and E47 cell lines and Dr. Anuradha Krishnan, Division of Gastroenterology and Hepatology, Mayo Clinic, Rochester is acknowledged for his help in scientific and language review of the manuscript. Financial assistance to first author (NUA) by University Grants Commission (UGC), New Delhi, India, is acknowledged. Dr. Shashi Bhushan is acknowledged for his help with flow cytometry experiments. Dr. Subash Bhardwaj is acknowledged for his help in histopathological analysis. Dr. P.R. Sharma is acknowledged for his help in confocal microscopy.

Conflict of Interest: The authors declare no conflict of interest.

Specific author contribution: **Ashraf Ul Nissar** maintained the cell cultures and performed cytotoxicity studies, Flow cytometry and western blotting studies and contributed in writing the manuscript. **Love sharma**

studied the blood parameters and maintained the animals**. Sheikh A Tasduq** formulated the research question, obtained the funding for the project, supervised the research and contributed in writing and editing of the manuscript.

Financial Support: UGC and CSIR, New Delhi, India

References:

1. N. D. Palmer, S. K. Musani, L. M. Yerges-Armstrong, M. F. Feitosa, L. F. Bielak, R. Hernaez, B. Kahali, J. J. Carr, T. B. Harris, M. A. Jhun, S. L. Kardia, C. D. Langefeld, T. H. Mosley, Jr., J. M. Norris, A. V. Smith, H. A. Taylor, L. E. Wagenknecht, J. Liu, I. B. Borecki, P. A. Peyser and E. K. Speliotes, *Hepatology*, 2013.
2. M. R. Charlton, J. M. Burns, R. A. Pedersen, K. D. Watt, J. K. Heimbach and R. A. Dierkhising, *Gastroenterology*, 2011, **141**, 1249-1253.
3. M. S. Ascha, I. A. Hanouneh, R. Lopez, T. A. Tamimi, A. F. Feldstein and N. N. Zein, *Hepatology*, 2010, **51**, 1972-1978.
4. N. Anderson and J. Borlak, *Pharmacol Rev*, 2008, **60**, 311-357.
5. Z. Z. Li, M. Berk, T. M. McIntyre and A. E. Feldstein, *J Biol Chem*, 2009, **284**, 5637-5644.
6. L. P. Bechmann, R. K. Gieseler, J. P. Sowa, A. Kahraman, J. Erhard, I. Wedemeyer, B. Emons, C. Jochum, T. Feldkamp, G. Gerken and A. Canbay, *Liver Int*, 2010, **30**, 850-859.
7. A. Bloch-Damti and N. Bashan, *Antioxid Redox Signal*, 2005, **7**, 1553-1567.
8. B. J. Song, R. L. Veech and P. Saenger, *J Clin Endocrinol Metab*, 1990, **71**, 1036-1040.
9. Z. Wang, S. D. Hall, J. F. Maya, L. Li, A. Asghar and J. C. Gorski, *Br J Clin Pharmacol*, 2003, **55**, 77-85.
10. L. Knockaert, B. Fromenty and M. A. Robin, *FEBS J*, 2011, **278**, 4252-4260.
11. P. S. Brookes, Y. Yoon, J. L. Robotham, M. W. Anders and S. S. Sheu, *Am J Physiol Cell Physiol*, 2004, **287**, C817-833.
12. C. M. Mayer and D. D. Belsham, *Endocrinology*, 2010, **151**, 576-585.
13. H. Puthalakath, L. A. O'Reilly, P. Gunn, L. Lee, P. N. Kelly, N. D. Huntington, P. D. Hughes, E. M. Michalak, J. McKimm-Breschkin, N. Motoyama, T. Gotoh, S. Akira, P. Bouillet and A. Strasser, *Cell*, 2007, **129**, 1337-1349.
14. H. Yamaguchi and H. G. Wang, *J Biol Chem*, 2004, **279**, 45495-45502.
15. W. Yoo, K. H. Noh, J. H. Ahn, J. H. Yu, J. A. Seo, S. G. Kim, K. M. Choi, S. H. Baik, D. S. Choi, T. W. Kim, H. J. Kim and N. H. Kim, *J Cell Biochem*, 2014, **115**, 1147-1158.
16. S. H. Ibrahim, Y. Akazawa, S. C. Cazanave, S. F. Bronk, N. A. Elmi, N. W. Werneburg, D. D. Billadeau and G. J. Gores, *J Hepatol*, 2011, **54**, 765-772.
17. G. Kanuri and I. Bergheim, *Int J Mol Sci*, 2013, **14**, 11963-11980.
18. M. Charlton, A. Krishnan, K. Viker, S. Sanderson, S. Cazanave, A. McConico, H. Masuoko and G. Gores, *Am J Physiol Gastrointest Liver Physiol*, 2011, **301**, G825-834.
19. A. A. Caro and A. I. Cederbaum, *Mol Pharmacol*, 2001, **60**, 742-752.
20. C. Pepper, A. Thomas, H. Tucker, T. Hoy and P. Bentley, *Leuk Res*, 1998, **22**, 439-444.
21. M. R. Farrukh, U. A. Nissar, Q. Afnan, R. A. Rafiq, L. Sharma, S. Amin, P. Kaiser, P. R. Sharma and S. A. Tasduq, *J Dermatol Sci*, 2014, **75**, 24-35.
22. M. Salido, J. L. Gonzalez and J. Vilches, *Mol Cancer Ther*, 2007, **6**, 1292-1299.
23. H. Malhi, S. F. Bronk, N. W. Werneburg and G. J. Gores, *J Biol Chem*, 2006, **281**, 12093-12101.
24. S. H. Tan, G. Shui, J. Zhou, Y. Shi, J. Huang, D. Xia, M. R. Wenk and H. M. Shen, *Autophagy*, 2014, **10**, 226-242.
25. M. Charlton, R. Sreekumar, D. Rasmussen, K. Lindor and K. S. Nair, *Hepatology*, 2002, **35**, 898-904.
26. M. W. Bradbury and P. D. Berk, *Clin Liver Dis*, 2004, **8**, 639-671, xi.
27. C. C. Shoulders and G. S. Shelness, *Curr Top Med Chem*, 2005, **5**, 283-300.
28. T. Sugimoto, S. Yamashita, M. Ishigami, N. Sakai, K. Hirano, M. Tahara, K. Matsumoto, T. Nakamura and Y. Matsuzawa, *J Hepatol*, 2002, **36**, 157-162.
29. G. Perlemuter, A. Sabile, P. Letteron, G. Vona, A. Topilco, Y. Chretien, K. Koike, D. Pessayre, J. Chapman, G. Barba and C. Brechot, *FASEB J*, 2002, **16**, 185-194.

30. P. Letteron, A. Sutton, A. Mansouri, B. Fromenty and D. Pessayre, *Hepatology*, 2003, **38**, 133-140.
31. R. V. Rao, H. M. Ellerby and D. E. Bredesen, *Cell Death Differ*, 2004, **11**, 372-380.
32. D. Ron and P. Walter, *Nat Rev Mol Cell Biol*, 2007, **8**, 519-529.
33. S. C. Cazanave, N. A. Elmi, Y. Akazawa, S. F. Bronk, J. L. Mott and G. J. Gores, *Am J Physiol Gastrointest Liver Physiol*, 2010, **299**, G236-243.
34. R. T. Waldron, A. D. Short, J. J. Meadows, T. K. Ghosh and D. L. Gill, *J Biol Chem*, 1994, **269**, 11927-11933.
35. T. Leung, R. Rajendran, S. Singh, R. Garva, M. Krstic-Demonacos and C. Demonacos, *Breast Cancer Res*, 2013, **15**, R107.
36. E. E. Hennig, M. Mikula, K. Goryca, A. Paziewska, J. Ledwon, M. Nesteruk, M. Woszczynski, B. Walewska-Zielecka, K. Pysniak and J. Ostrowski, *J Cell Mol Med*, 2014.
37. A. A. Caro and A. I. Cederbaum, *Arch Biochem Biophys*, 2002, **408**, 162-170.

Legends to figures:

Figure 1:

Fat accumulation, Cytotoxicity and NAFLD characteristic in hepatocytes and HC/HF mice: A: Nile red staining**. B:** The Cytotoxicity/Cell viability as mentioned. An asterisk (*) indicates a statistical difference (p<0.05) compared with unexposed (Control) cells. **C**: Palmitate induced lipotoxicity in C34 and E47 cell lines **D:** hep3B. Huh7 and HepG2 treated with Palmitic acid for 24 hours showed differential expression of Stearoyl-CoA desaturase1. **E:** Increased body weight and altered serum biochemistry in mice fed with HC/HF as compared to standard chow mice. **F:** Representative images (100X) of H&E and Picro sirus red stained sections of liver tissue from SC and HC/HF animals. No steatosis was observed in mice fed with SC. HC/HF mice showed micro and macro vesicular diffused steatosis, hepatocyte ballooning (indicated by arrows in image B), infiltration of neutrophils (Steatohepatitis, as indicated by arrows in the image C), prominence of Kupffer cells (as indicated by arrows in E) and there were little or no signs of signs of collagen deposition.

Figure 2:

Effect of Palmitic acid on the protein expression of SREBP1, CD36, PPARγ and Mttp in hepatocytes and HC/HF mice (Lipid droplet formation machinery): **A:** Huh7, Hep3B, HepG2 cells were incubated in presence or absence of Palmitic acid for 24 hours. Whole cell lysates were resolved by SDS-PAGE transferred to PVDF membrane and immunoblotted with indicated antibodies. Detection of bands was done by enhanced chemiluminiscence. Graphical data of blots represents the arbitrary units in the intensity of individual bands. Images shown are representative blots. **B:** Expression of different proteins in the livers of SC and HC/HF mice. An asterisk (*) indicates a statistical difference (p<0.05) compared with control

Figure 3: Effect of Palmitic acid on intracellular Ca^{2+} and PERK-eIF2α pathway in hepatocytes: **3A):** Hep3B and Huh7 cells were incubated in presence or abscence of Palmitic acid for 4 hours. Cells were incubated with 5μM Fluo3-AM for 30 minutes. Cells were washed with PBS and slides were prepared for Confocal microscopy and imaging was done using laser scanning confocal microscope. Five random microscopic fields were selected. Images shown are representative. Quantification of intensity was done by fluoview FV-1000 software. * indicates p<0.05 and is considered as statistically significant**. 3B):** Huh7 and Hep3B cells were incubated in presence or absence of Palmitic acid for 12 hours. Thapsigargin was used as positive control for ER stress induction. Whole cell lysates were resolved by SDS-PAGE transferred to PVDF membrane and immunoblotted with indicated antibodies. Detection of bands was done by enhanced chemiluminiscence. Images shown are representative blots. **3C)** Bar chart representing the densitometry of corresponding blots in Hep3B and HuH7. An asterisk (*) indicates a statistical difference (p<0.05) compared with control. **3D**) Cell viability analysis under ER stress inhibited conditions in palmitate treated cells. Cells were pretreated with 4-Phenylbutyric acid 4 hours prior to palmitate treatment and cellular viability was assessed after 24 hours by MTT assay.

Figure 4:

Effect of Palmitic acid on the mitochondrial membrane potential in hepatocytes: JC-1 staining as mentioned in Materials and Methods section. Five random microscopic fields were selected. Images shown are representative. An asterisk (*) indicates a statistical difference (p<0.05) compared with control

Figure 5:

Reactive Oxygen Species and CYP2E1 : A: H_2DCFH-DA staining as mentioned. **B):** Intensity measurements of ROS using ImageJ software. C & D):Analysis of Anti oxidant defense/response system (ARE) in palmitate treated cells 24 hour after treatment E & F) :CYP2E1 expression in Hep3B, HepG2 and Huh7 cells 24 hours post Palmitic acid exposure. G & H): Densitometric analysis of CYP2E1 in livers of mice (Control and HC/HF). * indicates p<0.05 and is considered as statistically significant

Figure 6:

Effect of Palmitic acid on the expression of apoptotic markers in hepatocytes: Huh7, Hep3B and HepG2 cells were incubated in presence or absence of Palmitic acid for 24 hours. Whole cell lysates were resolved by SDS-PAGE transferred to PVDF membrane and immunoblotted with indicated antibodies. Detection of bands was done by enhanced chemiluminiscence. Images shown are representative blots. The bar charts represent the PARP cleavage in Hep3B and HuH7 cells.

Figure 7:

Proposed pathogenic link between fat transport and cellular injury.

Supplement Figure 1:

Detailed composition of high cholesterol and high fat diet used in the *in vivo* model of NAFLD.

Supplement Figure 2:

CYP2E1 expression C34 and E47 cells and cytotoxicity induced by palmitic acid in AML12 cells

Supplement Figure 3: Supplement Figure 3: IL-6 release in Hep3B cells: (*) indicates p<0.05 and is considered as statistically significant

Figure 1

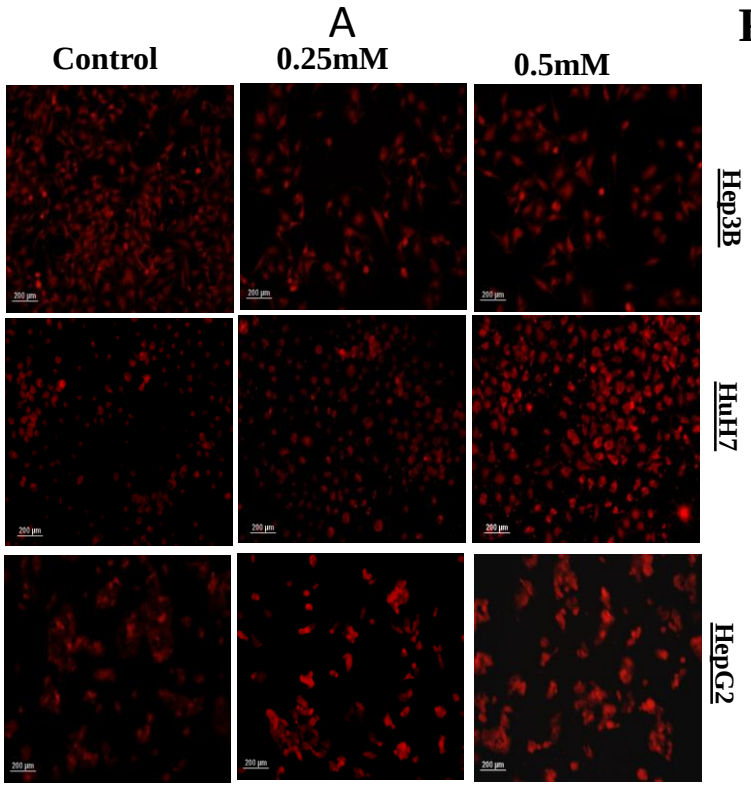
A
Control
0.25mM
0.5mM
Hep3B
HuH7
HepG2

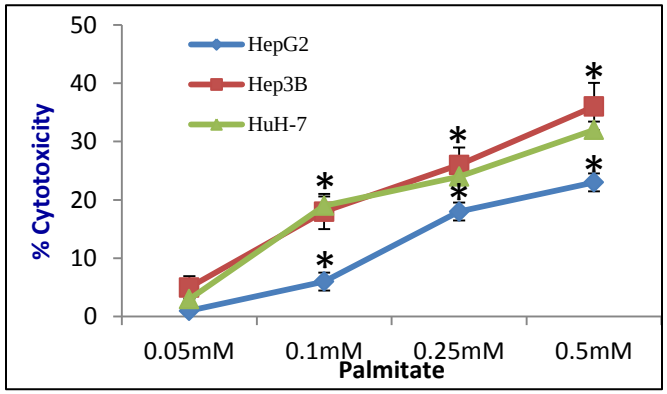
B
% Cytotoxicity
HepG2
Hep3B
HuH-7
0.05mM
0.1mM
0.25mM
0.5mM
Palmitate

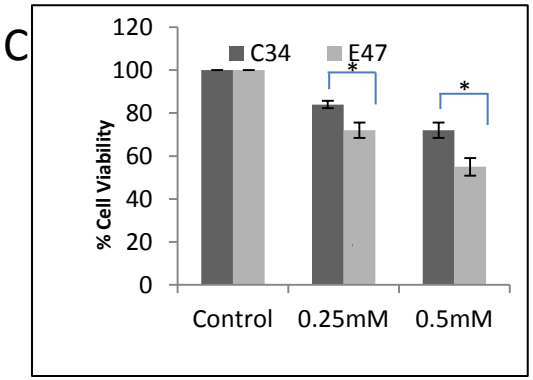
C
% Cell Viability
C34
F47
Control
0.25mM
0.5mM

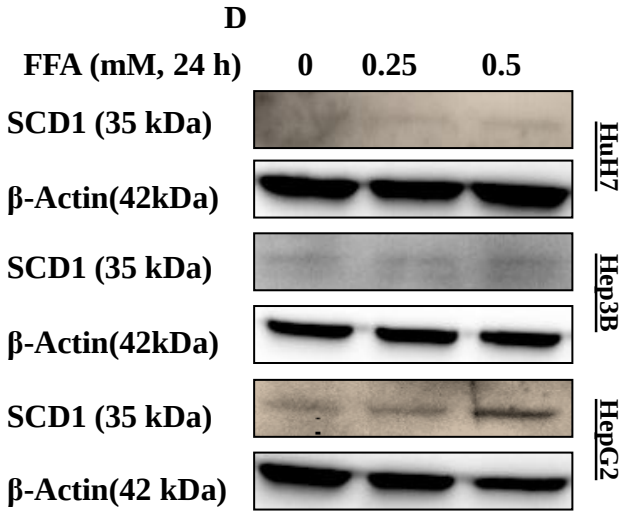
D
FFA (mM, 24 h)
0
0.25
0.5
SCD1 (35 kDa)
β-Actin(42kDa)
HuH7
SCD1 (35 kDa)
β-Actin(42kDa)
Hep3B
SCD1 (35 kDa)
β-Actin(42 kDa)
HepG2

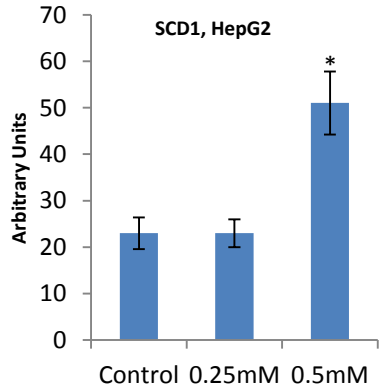
SCD1, HepG2
Arbitrary Units
Control
0.25mM
0.5mM

1E

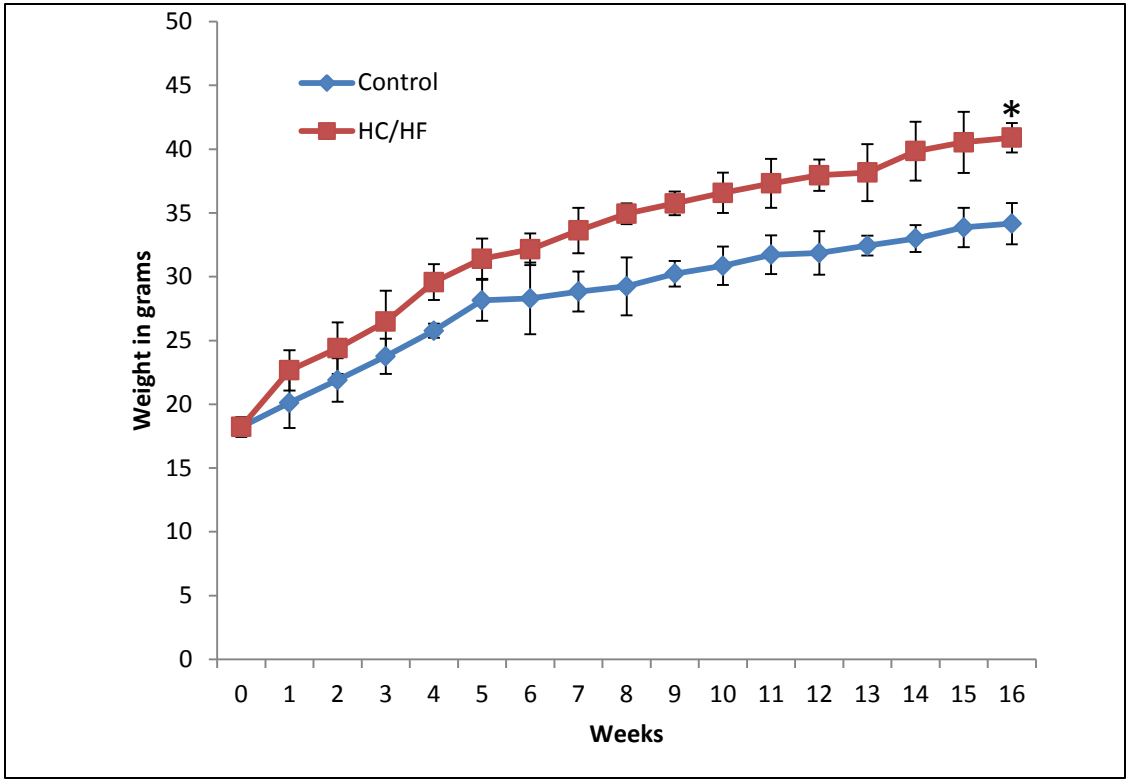
Control
HC/HF
Weight in grams
Weeks
*

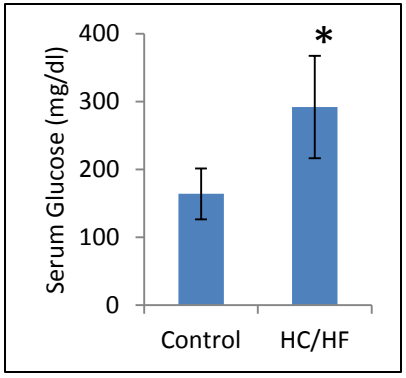
Serum Glucose (mg/dl)
Control
HC/HF
*

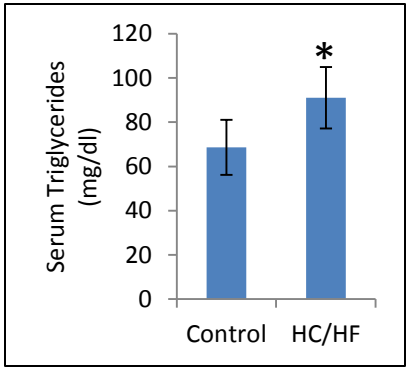
Serum Triglycerides (mg/dl)
Control
HC/HF
*

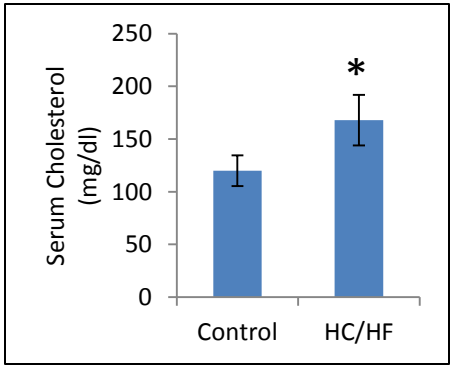
Serum Cholesterol (mg/dl)
Control
HC/HF
*

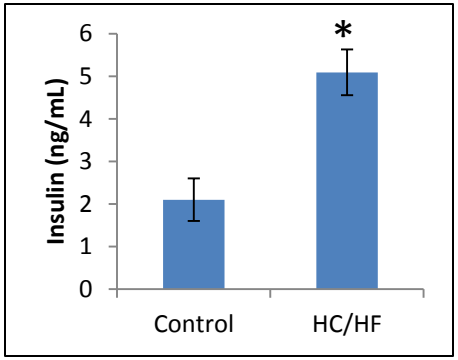
Insulin (ng/mL)
Control
HC/HF
*

1F

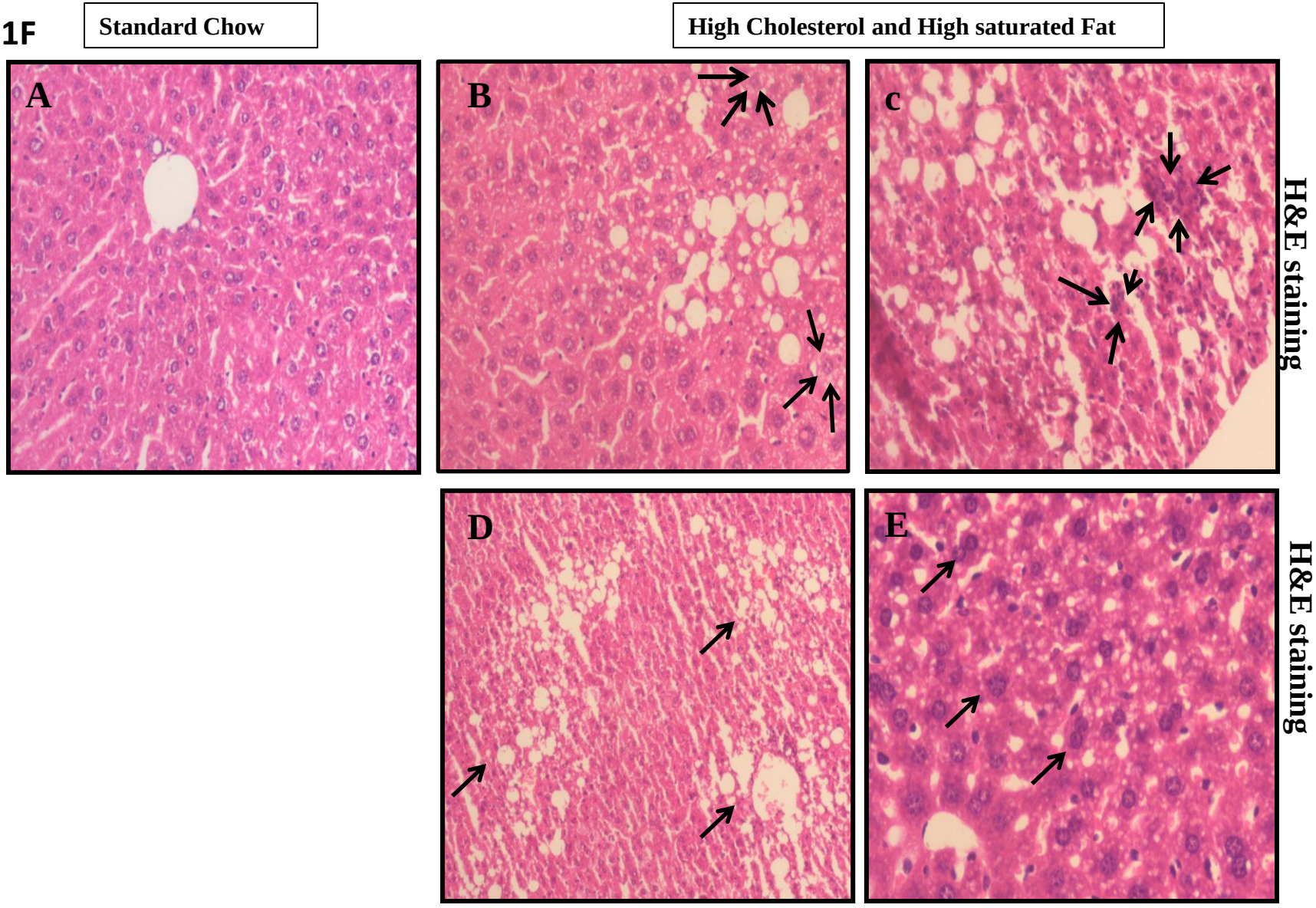
Standard Chow
High Cholesterol and High saturated Fat
A
B
c
D
E
H&E staining
H&E staining

Huh7

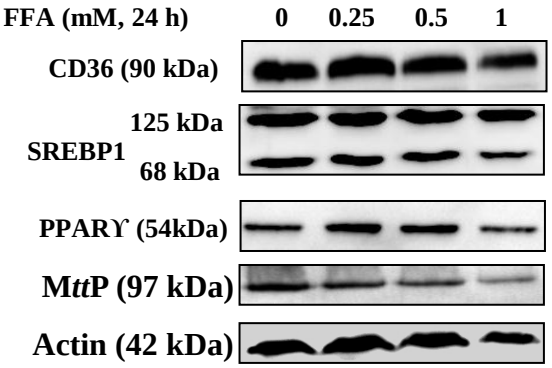

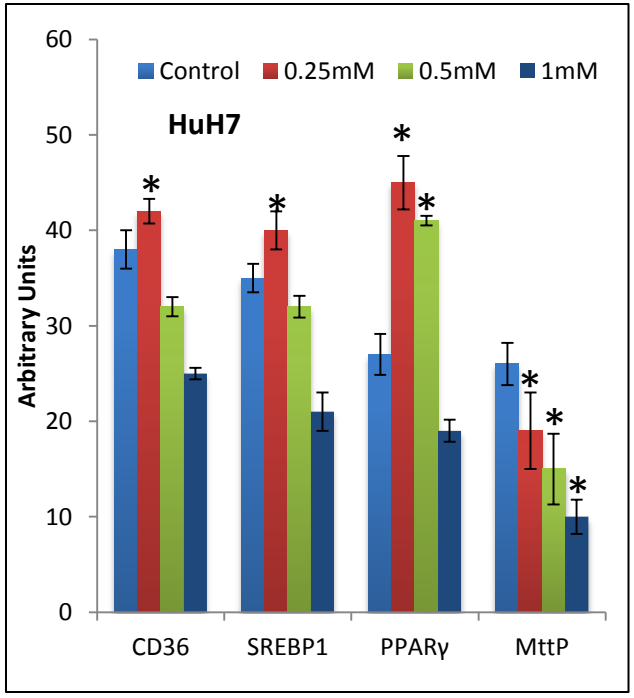

Hep3B

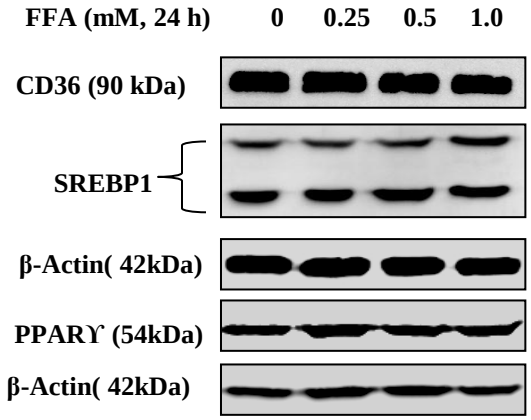

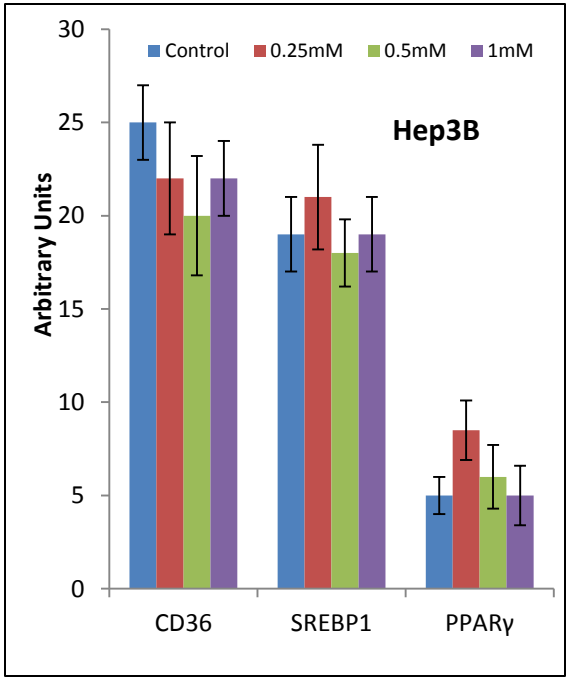

HepG2

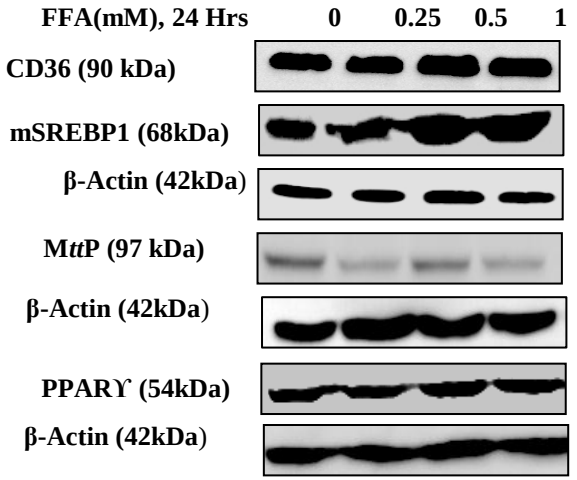

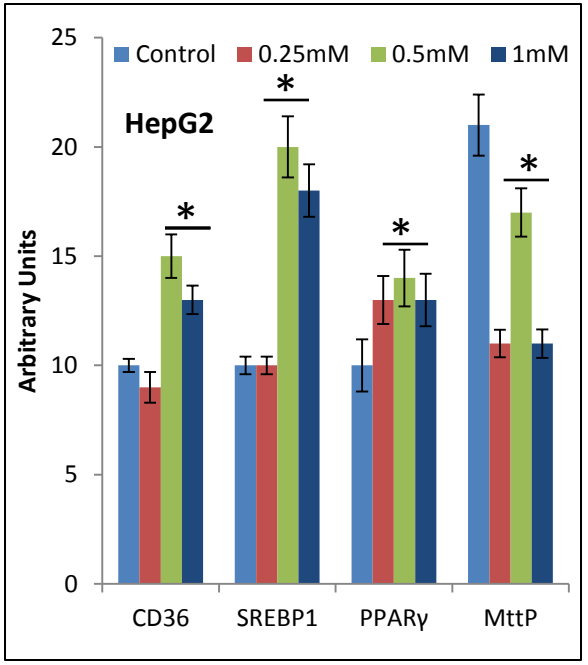

Figure 2B

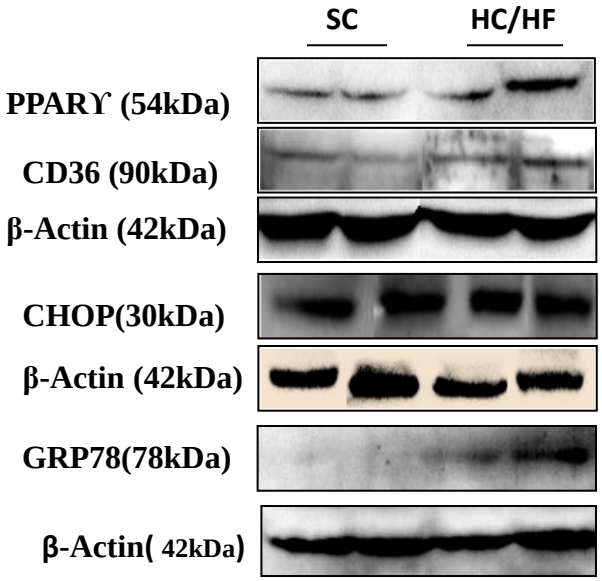
SC
HC/HF
PPARϒ (54kDa)
CD36 (90kDa)
β-Actin (42kDa)
CHOP(30kDa)
β-Actin (42kDa)
GRP78(78kDa)
β-Actin(42kDa)

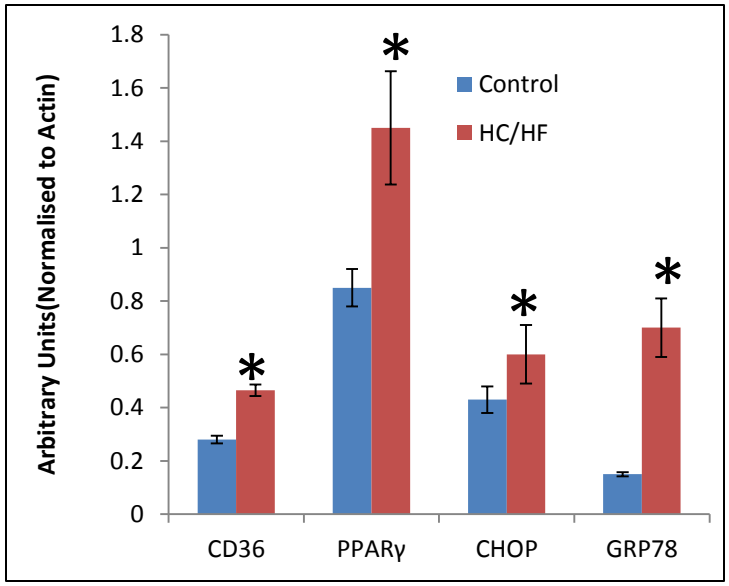
Arbitrary Units(Normalised to Actin)
1.8
1.6
1.4
1.2
1
0.8
0.6
0.4
0.2
0
Control
HC/HF
*
*
*
*
CD36
PPARγ
CHOP
GRP78

Figure 3

A

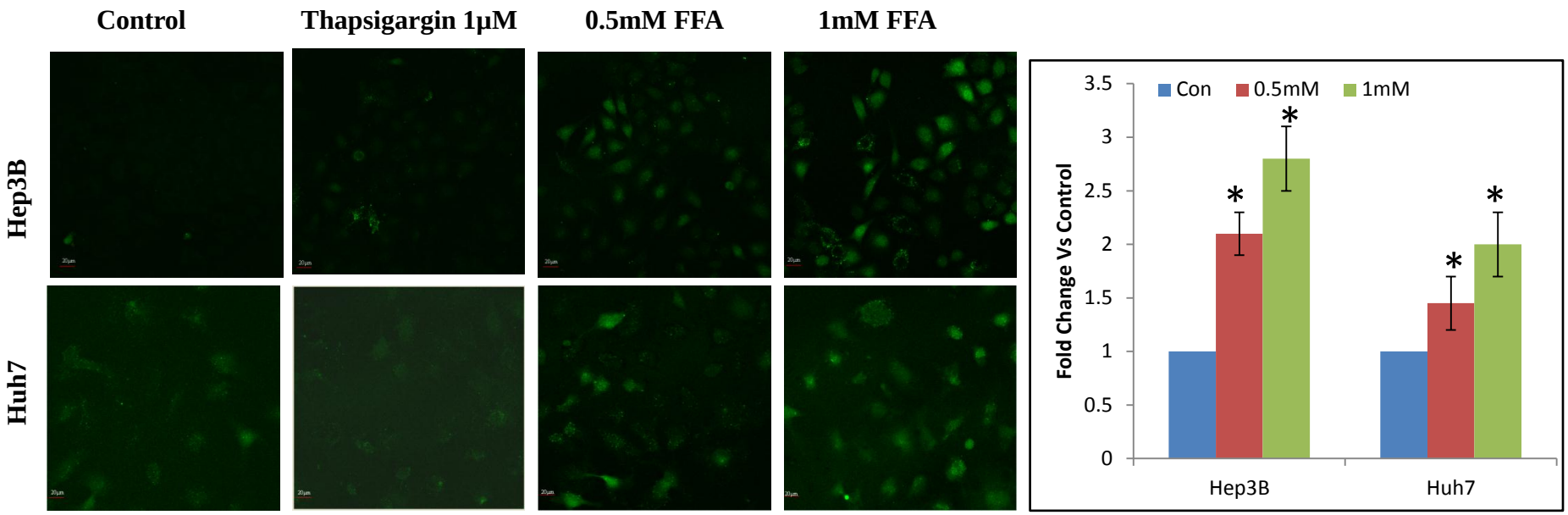
Control
Thapsigargin 1μM
0.5mM FFA
1mM FFA
Hep3B
Huh7
Con
0.5mM
1mM
Fold Change Vs Control
3.5
3
2.5
2
1.5
1
0.5
0
Hep3B
Huh7

B

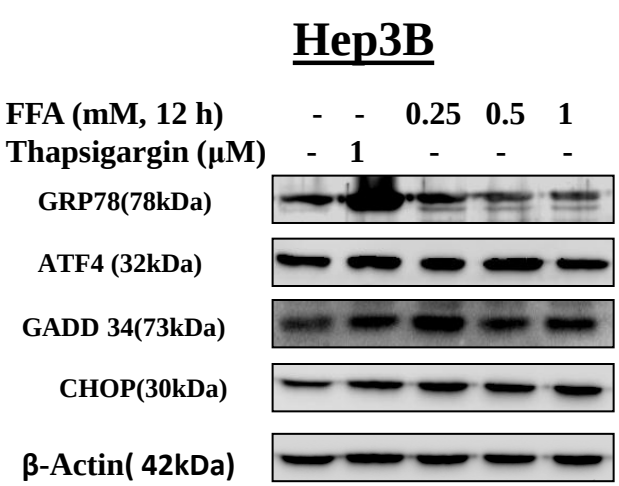
Hep3B
FFA (mM, 12 h) - - 0.25 0.5 1
Thapsigargin (μM) - 1 - - -
GRP78(78kDa)
ATF4 (32kDa)
GADD 34(73kDa)
CHOP(30kDa)
β-Actin(42kDa)

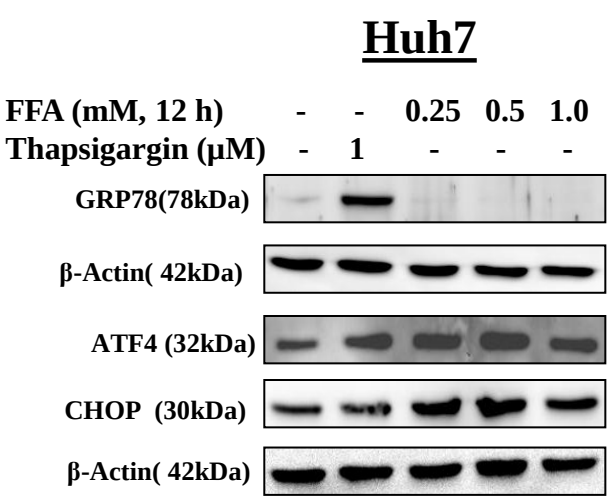
Huh7
FFA (mM, 12 h) - - 0.25 0.5 1.0
Thapsigargin (μM) - 1 - - -
GRP78(78kDa)
β-Actin(42kDa)
ATF4 (32kDa)
CHOP (30kDa)
β-Actin(42kDa)

D

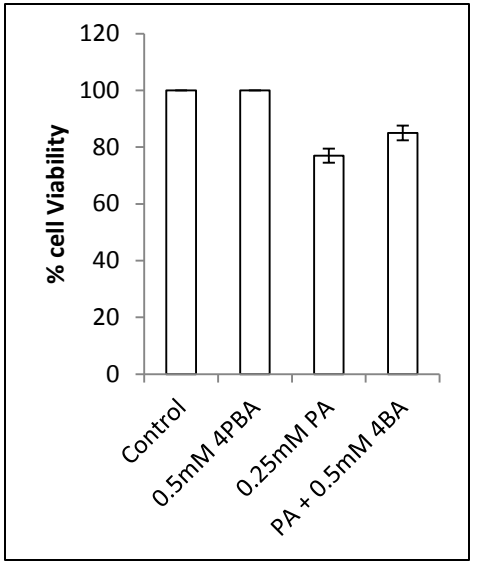
% cell Viability
120
100
80
60
40
20
0
Control
0.5mM 4PBA
0.25mM PA
PA + 0.5mM 4BA

C

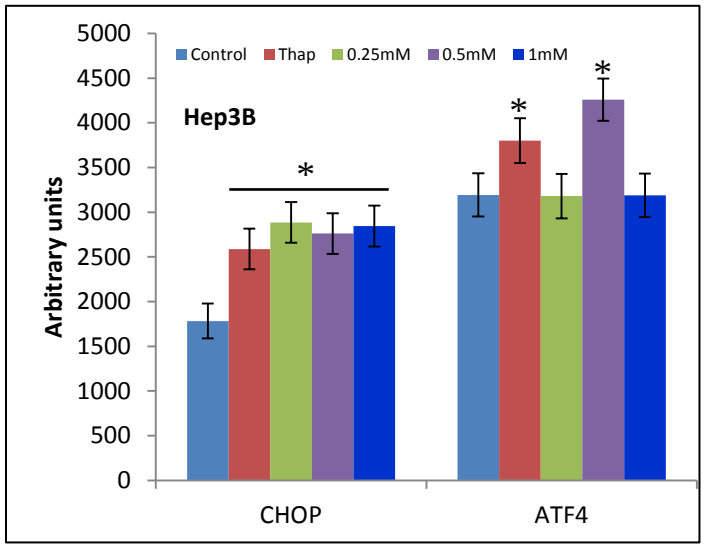
Hep3B
Control
Thap
0.25mM
0.5mM
1mM
Arbitrary units
5000
4500
4000
3500
3000
2500
2000
1500
1000
500
0
CHOP
ATF4

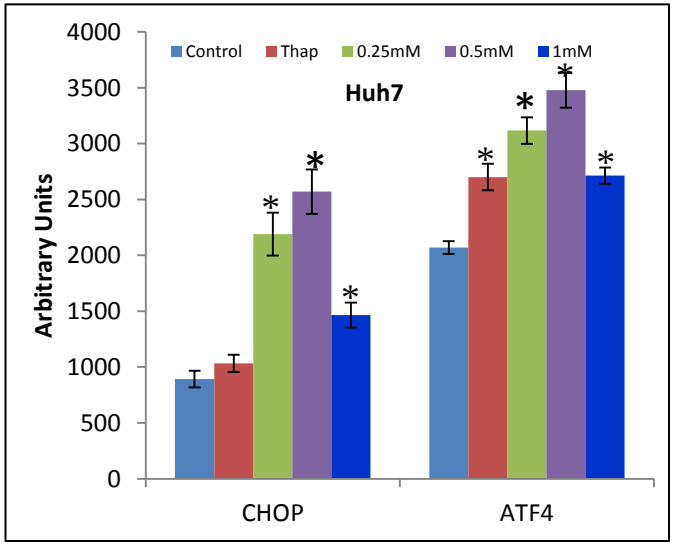
Huh7
Control
Thap
0.25mM
0.5mM
1mM
Arbitrary Units
4000
3500
3000
2500
2000
1500
1000
500
0
CHOP
ATF4

Figure 4

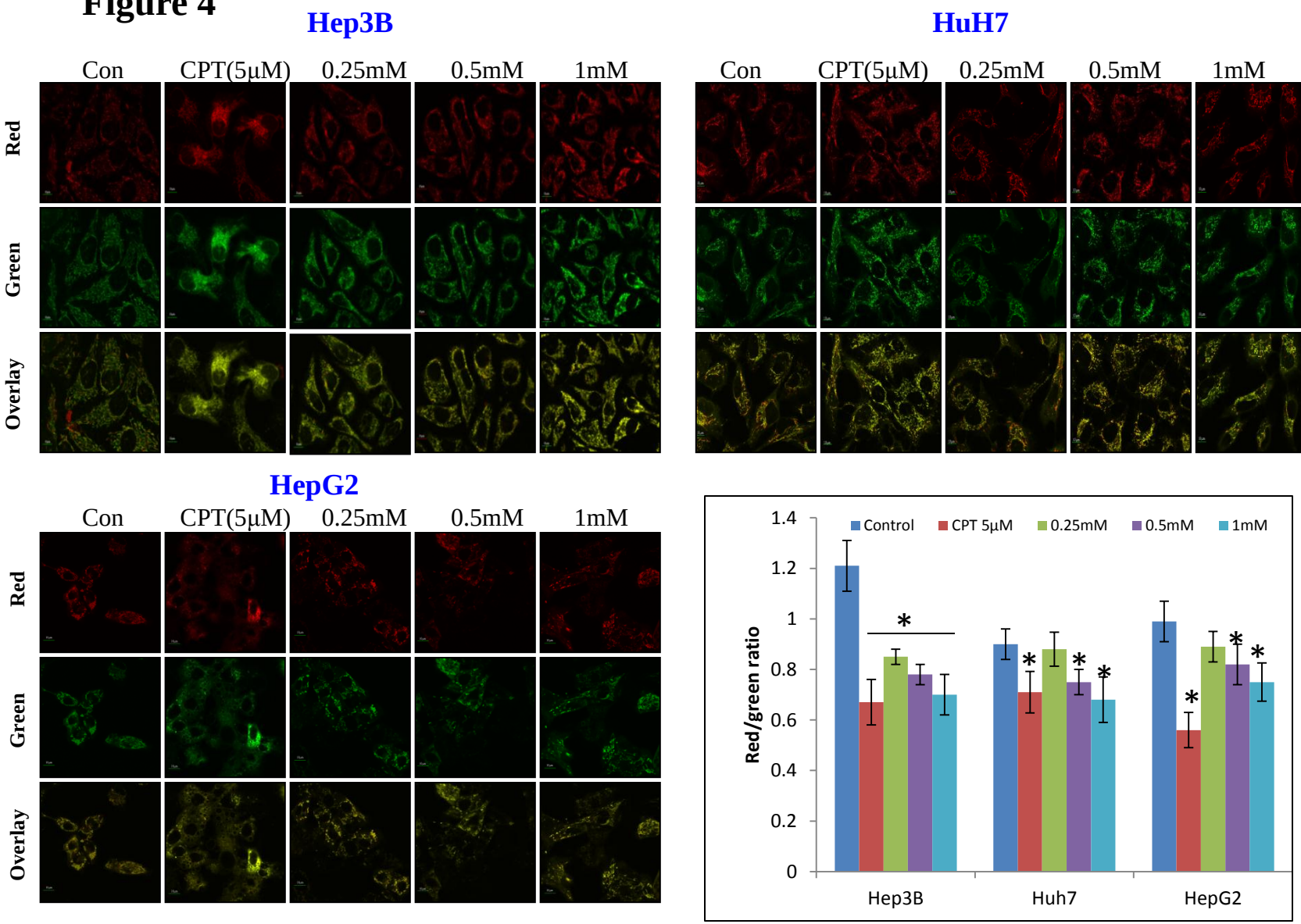
Hep3B
HuH7
HepG2
Con
CPT(5μM)
0.25mM
0.5mM
1mM
Red
Green
Overlay
Control
CPT 5μM
0.25mM
0.5mM
1mM
Red/green ratio
1.4
1.2
1
0.8
0.6
0.4
0.2
0
Hep3B
Huh7
HepG2

Figure 5

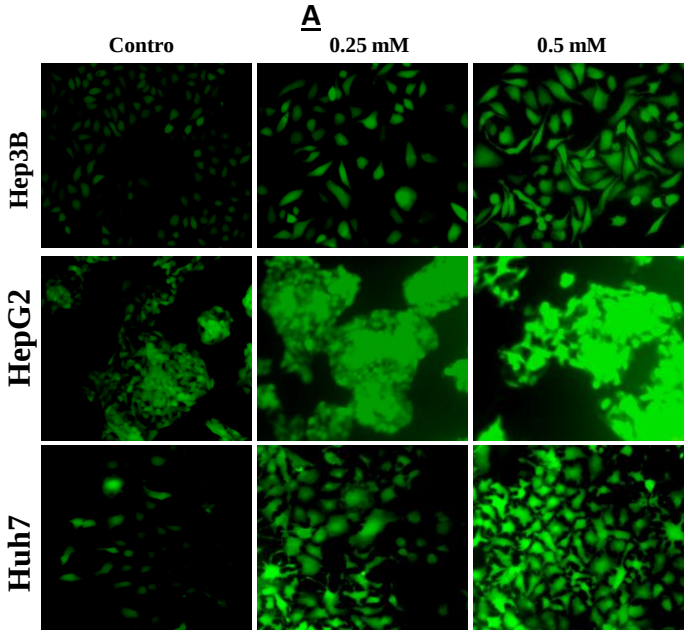
A
Contro
0.25 mM
0.5 mM
Hep3B
HepG2
Huh7

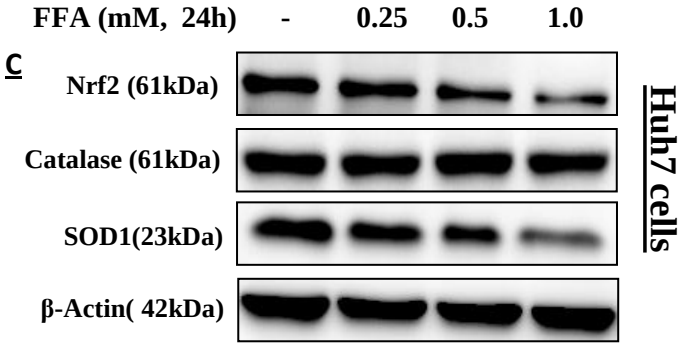
FFA (mM, 24h) - 0.25 0.5 1.0
C
Nrf2 (61kDa)
Catalase (61kDa)
SOD1(23kDa)
β-Actin(42kDa)
Huh7 cells

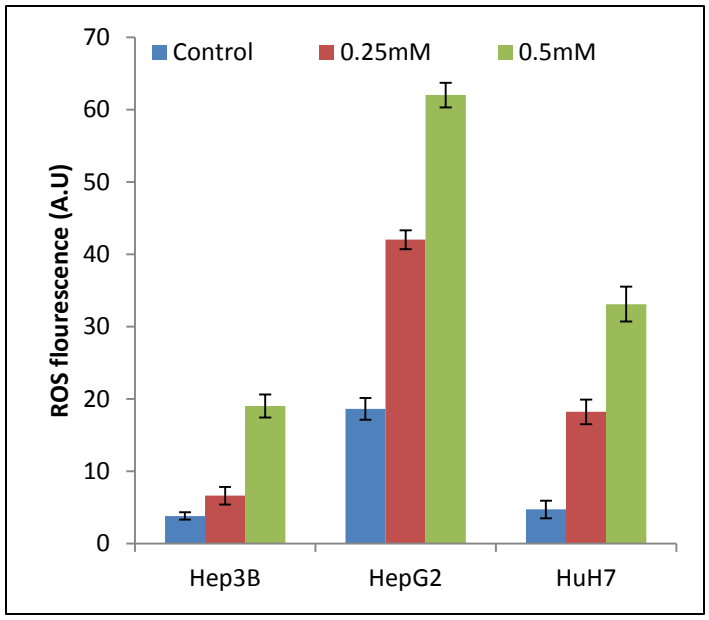
B
Control
0.25mM
0.5mM
ROS flourescence (A.U)
70
60
50
40
30
20
10
0
Hep3B
HepG2
HuH7

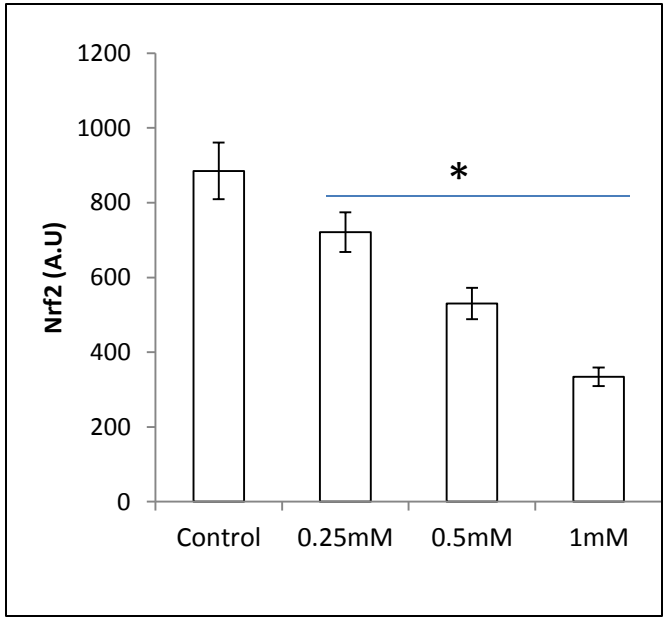
D
Nrf2 (A.U)
1200
1000
800
600
400
200
0
*
Control
0.25mM
0.5mM
1mM

E

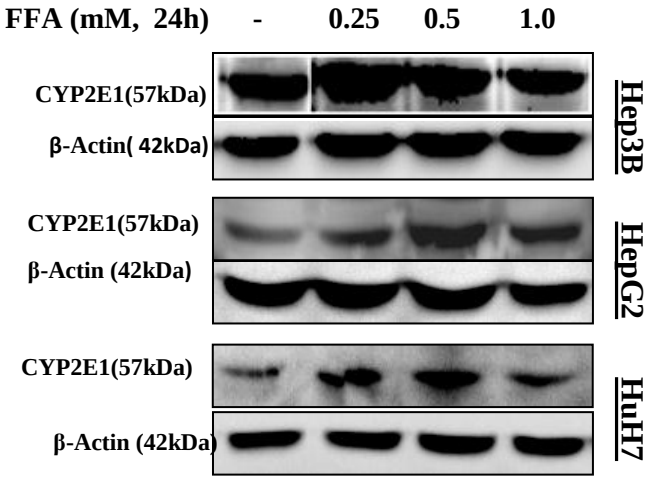
FFA (mM, 24h) - 0.25 0.5 1.0
CYP2E1(57kDa)
β-Actin(42kDa)
Hep3B
CYP2E1(57kDa)
β-Actin (42kDa)
HepG2
CYP2E1(57kDa)
β-Actin (42kDa)
HuH7

G

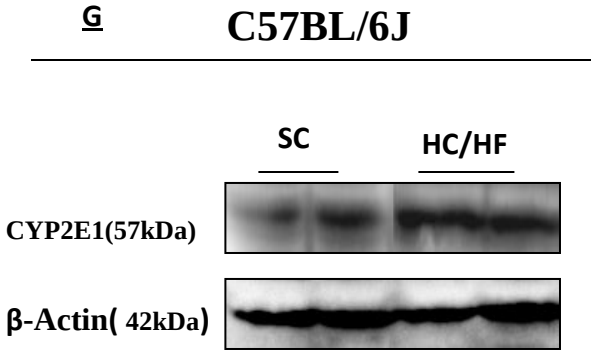
C57BL/6J
SC
HC/HF
CYP2E1(57kDa)
β-Actin(42kDa)

F

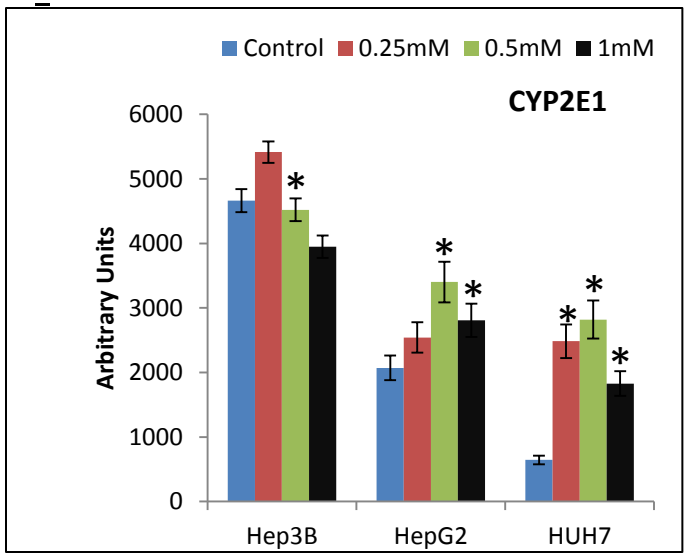
Control
0.25mM
0.5mM
1mM
CYP2E1
Arbitrary Units
6000
5000
4000
3000
2000
1000
0
Hep3B
HepG2
HUH7

H

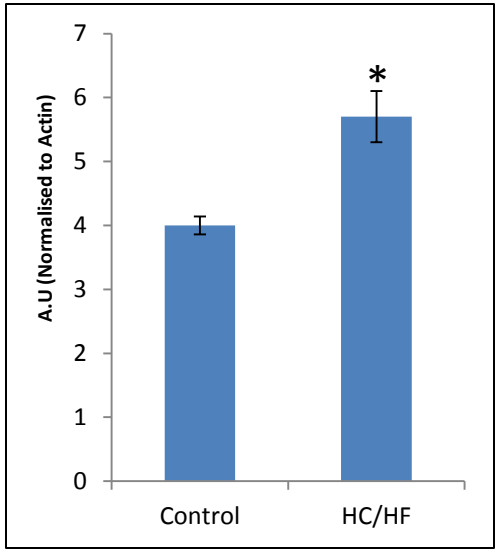
A.U (Normalised to Actin)
7
6
5
4
3
2
1
0
Control
HC/HF

Figure 6

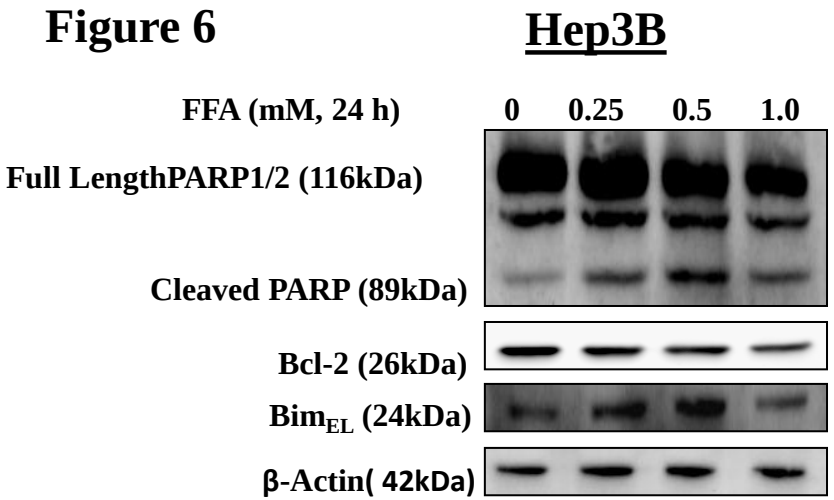
Hep3B
FFA (mM, 24 h)
0
0.25
0.5
1.0
Full LengthPARP1/2 (116kDa)
Cleaved PARP (89kDa)
Bcl-2 (26kDa)
Bim$_{EL}$ (24kDa)
β-Actin(42kDa)

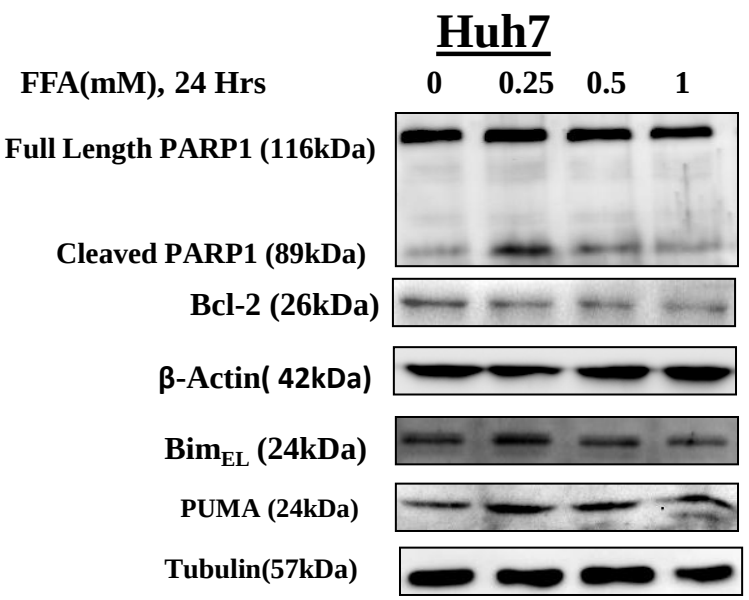
Huh7
FFA(mM), 24 Hrs
0
0.25
0.5
1
Full Length PARP1 (116kDa)
Cleaved PARP1 (89kDa)
Bcl-2 (26kDa)
β-Actin(42kDa)
Bim$_{EL}$ (24kDa)
PUMA (24kDa)
Tubulin(57kDa)

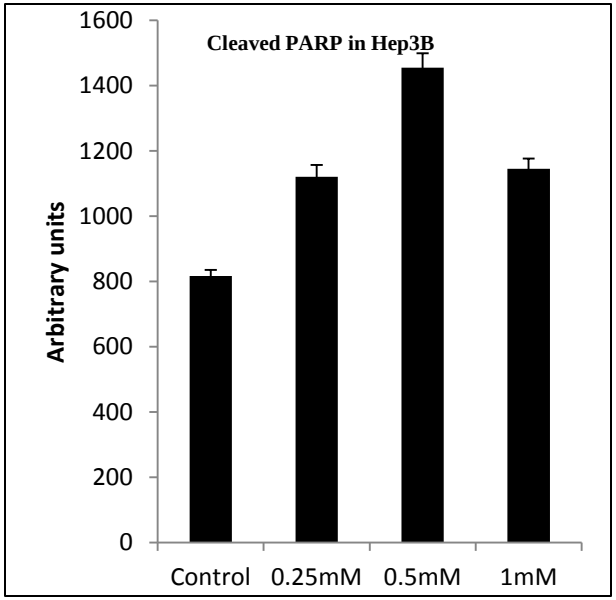
Cleaved PARP in Hep3B
Arbitrary units
1600
1400
1200
1000
800
600
400
200
0
Control
0.25mM
0.5mM
1mM

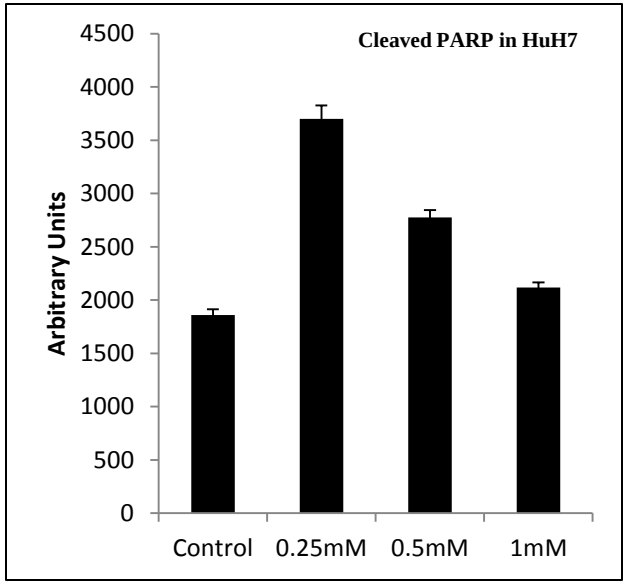
Cleaved PARP in HuH7
Arbitrary Units
4500
4000
3500
3000
2500
2000
1500
1000
500
0
Control
0.25mM
0.5mM
1mM

Figure 7

Circulating Free Fatty Acid (Obtained from dietary sources/insulin resistance)

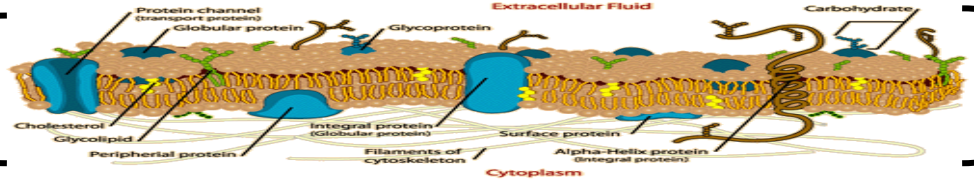

Cell Membrane

Hepatocyte

Free Fatty Acids within the cell leading to ROS → SCD1↑ → Triglyceride accumulation

Intracellular Ca^{2+} release

(SREBP1, CD36, PPARγ)↑, Mttp↓

ER Stress

Fat Accumulation (first Hit)/Lipogenesis

Apoptosis

ROS CYP2E1

NASH (Second Hit)